UCSF

Title

Levetiracetam suppresses neuronal network dysfunction and reverses synaptic and cognitive deficits in an Alzheimer's disease model.

Permalink

https://escholarship.org/uc/item/6z30k0q8

Journal

Proceedings of the National Academy of Sciences of the United States of America, 109(42)

ISSN

0027-8424

Authors

Sanchez, Pascal E
Zhu, Lei
Verret, Laure
et al.

Publication Date

2012-10-01

DOI

10.1073/pnas.1121081109

Peer reviewed

Levetiracetam suppresses neuronal network dysfunction and reverses synaptic and cognitive deficits in an Alzheimer's disease model

Pascal E. Sanchez[a,b], Lei Zhu[a,b], Laure Verret[a,b], Keith A. Vossel[a,b], Anna G. Orr[a,b], John R. Cirrito[c], Nino Devidze[a], Kaitlyn Ho[a], Gui-Qiu Yu[a], Jorge J. Palop[a,b], and Lennart Mucke[a,b,1]

[a]Gladstone Institute of Neurological Disease, San Francisco, CA 94158; [b]Department of Neurology, University of California, San Francisco, CA 94158; and [c]Department of Neurology, Washington University School of Medicine, St. Louis, MO 63110

Edited* by Richard L. Huganir, The Johns Hopkins University School of Medicine, Baltimore, MD, and approved July 11, 2012 (received for review December 21, 2011)

In light of the rising prevalence of Alzheimer's disease (AD), new strategies to prevent, halt, and reverse this condition are needed urgently. Perturbations of brain network activity are observed in AD patients and in conditions that increase the risk of developing AD, suggesting that aberrant network activity might contribute to AD-related cognitive decline. Human amyloid precursor protein (hAPP) transgenic mice simulate key aspects of AD, including pathologically elevated levels of amyloid-β peptides in brain, aberrant neural network activity, remodeling of hippocampal circuits, synaptic deficits, and behavioral abnormalities. Whether these alterations are linked in a causal chain remains unknown. To explore whether hAPP/amyloid-β–induced aberrant network activity contributes to synaptic and cognitive deficits, we treated hAPP mice with different antiepileptic drugs. Among the drugs tested, only levetiracetam (LEV) effectively reduced abnormal spike activity detected by electroencephalography. Chronic treatment with LEV also reversed hippocampal remodeling, behavioral abnormalities, synaptic dysfunction, and deficits in learning and memory in hAPP mice. Our findings support the hypothesis that aberrant network activity contributes causally to synaptic and cognitive deficits in hAPP mice. LEV might also help ameliorate related abnormalities in people who have or are at risk for AD.

epilepsy | plasticity | therapy | dementia | hyperexcitability

No effective therapies exist to prevent, halt, or reverse Alzheimer's disease (AD). Because the number of AD cases is predicted to rise to over 100 million worldwide by 2050 (1), the identification of such therapies is both important and urgent. A large body of work suggesting that amyloid-β (Aβ) peptides contribute causally to the pathogenesis of AD has resulted in the development of anti-Aβ therapies, some of which are being evaluated in advanced clinical trials (2–5). However, it is uncertain whether these treatment strategies will be efficacious and safe. In fact, strategies to block the production or enhance the clearance of Aβ have been associated with serious side effects that probably are unrelated to the reduction of Aβ levels per se (4, 6). Thus, it is desirable to identify alternative or complementary therapeutic strategies to block Aβ-induced neuronal dysfunction.

In this regard, it is interesting that perturbation of neuronal network activity may be a major and early contributor to AD pathogenesis (7). Aberrant neuronal network activity is observed in AD patients and in conditions that increase the risk of developing AD (7–11). AD patients have an increased incidence of epileptic seizures, and the incidence is highest in patients with early-onset AD who overexpress human amyloid precursor protein (hAPP) and Aβ as a result of hAPP gene duplication or trisomy 21 or who carry mutations that alter hAPP processing and Aβ production (7). Transgenic mice with neuronal expression of mutant APP have pathologically elevated levels of Aβ in AD-vulnerable brain regions and show epileptiform activity on EEG recordings as well as synaptic and cognitive deficits

(12–16). However, it remains uncertain if the aberrant network activity contributes to APP/Aβ-dependent synaptic and cognitive deficits and whether antiepileptic drugs can reverse these deficits. The current study addresses these questions.

Among multiple antiepileptic drugs tested, only levetiracetam (LEV) effectively suppressed abnormal spiking activity in hAPP mice. Chronic treatment with LEV also reversed their behavioral abnormalities, cognitive impairments, remodeling of hippocampal circuits, and synaptic deficits, suggesting that these alterations are causally linked to aberrant network activity.

Results

LEV Reduces Abnormal Spike Activity in hAPP Mice. hAPP mice from line J20 (hAPPJ20 mice) have pathologically elevated levels of human Aβ in the brain and show neuronal network dysfunction, including frequent abnormal spiking activity and more intermittent epileptic seizures (12, 15, 17). We used video-EEG recordings in freely moving hAPPJ20 mice to assess the effect of different Food and Drug Administration (FDA)-approved antiepileptic drugs on abnormal spiking activity. An abnormal spike was defined as a brief (<70 ms), high-voltage deflection on the EEG that was eightfold greater than the average baseline amplitude measured during the 5 s preceding the deflection. The number of spikes per hour on subdural EEG recordings was used as the main outcome measure. Nontransgenic (NTG) mice had no such abnormal spikes, whereas hAPP mice had ~12 spikes/h (Fig. 1A and B). Spikes were detected in the frontal and parietal cortices and in the hippocampus (Fig. S1A). The antiepileptic drugs ethosuximide, gabapentin, phenytoin, pregabalin, valproic acid, and vigabatrin, known for their antiepileptic efficacy in animal models and in humans with other types of epilepsy (18), did not reduce spike frequency significantly in hAPP mice (Table 1). Phenytoin actually increased abnormal spike activity in these mice, consistent with previous findings (17), and pregabalin had a similar effect. In contrast, LEV, a second-generation antiepileptic drug (19, 20), had potent antiepileptic effects in hAPP mice. A single injection of LEV rapidly and transiently reduced spike occurrence in the cortex and hippocampus in a dose-dependent manner (Fig. 1 A–D, Fig. S1 A and B, and Table 1). Saline injection did not modify the frequency of spikes (Fig. S2).

Table 1. Acute effects of different antiepileptic drugs in hAPPJ20 mice

FDA-approved antiepileptic drugs	Acute injection dose (mg/kg)	Fraction of mice with >50% spike reduction	Change in spikes relative to baseline (%)*	Statistical significance[†]	Effect
Ethosuximide	400	1/6	−0.8 (± 18.9)	$P = 0.96$	None
Gabapentin	100	0/4	−10.3 (± 12.1)	$P = 0.45$	None
Levetiracetam	200	7/7	−70.6 (± 4.9)	$P < 0.0001$	Suppression
Phenytoin	100	0/3	+183.2 (± 48.7)	$P = 0.043$	Exacerbation
Pregabalin	200	0/3	+87.7 (± 14.6)	$P = 0.026$	Exacerbation
Valproic acid	300	0/4	+20.3 (± 15.4)	$P = 0.28$	None
Vigabatrin	300	0/4	+0.8 (± 15.6)	$P = 0.96$	None

*Over a period of 6 h postinjection.
[†]One-sample t test compared to baseline.

We next explored whether chronic LEV treatment (75 mg·kg^{-1}·d^{-1}) could reduce abnormal spike activity persistently in hAPP mice. To infuse LEV chronically, osmotic minipumps were implanted subcutaneously (s.c.). Plasma levels of LEV were stable throughout the duration of the infusion (28 d) and were almost undetectable 12 d after the end of the infusion (Fig. 1E).

Spike frequency was measured from the parietal cortex before (baseline) and repeatedly during continuous infusion of LEV. This treatment persistently reduced abnormal spike activity to ~50% of baseline levels in hAPP mice (Fig. 1F), indicating that mice did not develop resistance to the effect of LEV at this dose and that LEV effectively suppressed epileptiform discharges in hAPP
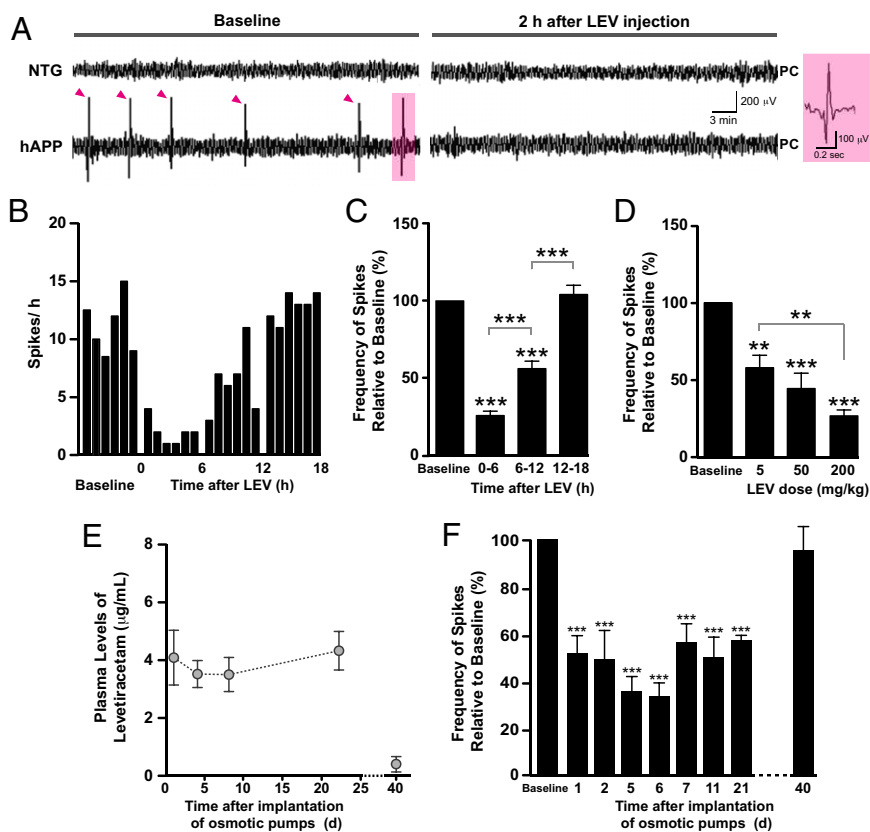

Fig. 1. LEV decreases abnormal spike activity in hAPP mice acutely and chronically. Subdural EEG activity from parietal cortices (PC) was recorded in NTG (n = 3) and hAPPJ20 (n = 16) mice before and after LEV administration. (A) Representative recordings showing typical EEG patterns in NTG and hAPP mice. hAPP mice displayed frequent epileptiform spikes (marked by magenta arrowheads). Acute LEV injection (200 mg/kg, i.p.) transiently suppressed these abnormal events in hAPP mice as illustrated by the suppression of spikes in an hAPP mouse 2 h after LEV injection. Right panel shows details of a high-voltage biphasic spike shaded in magenta on the left. (B) Time course of the LEV effect in the same hAPP mouse. Each bar represents the total number of epileptiform spikes per hour. (C) Baseline EEGs were recorded for 24 h, and drugs were injected at the end of this recording period. During the first 6 h after the injection, LEV reduced the number of epileptiform spikes in hAPP mice (n = 16) by ~75% on average. Subsequently, the frequency of epileptiform spikes increased gradually, returning to baseline levels by 12–18 h after the injection. (D) Dose-dependent effect of LEV on spike frequency during the first 6 h after the injection (n = 5–6 hAPP mice per dose). (E) Plasma concentration of LEV in hAPP mice (n = 4) determined during and after chronic infusion of the drug (75 mg·kg^{-1}·d^{-1}) by s.c. implanted osmotic minipumps. (F) EEGs were recorded in hAPP mice (n = 10) 24 h before (baseline), during, and after continuous infusion of LEV (75 mg·kg^{-1}·d^{-1}) for 28 d. Spike frequencies were reduced to ~50% of baseline levels throughout the LEV infusion and returned to baseline level by 12 d after the end of the treatment. **$P < 0.005$, ***$P < 0.0005$ vs. baseline or as indicated by brackets (one-way ANOVA and Bonferroni test). Values in C–F are means ± SEM.

mice. Spike frequency returned to baseline levels 2 wk after cessation of the treatment (Fig. 1F).

Chronic LEV Treatment Reverses Behavioral Abnormalities in hAPP Mice. Like other APP transgenic lines, hAPPJ20 mice are hyperactive in the open field (21, 22) and spend more time than NTG mice in the open arms in the elevated plus maze (21, 23, 24). Prescreening of untreated mice in an open field at 2.5–3.0 mo of age confirmed the hyperactivity of hAPP mice (Fig. 2A). Mice were then divided into groups so that baseline activity levels did not differ between genotype-matched groups that received saline or LEV (Fig. 2B). hAPP mice and NTG controls were tested during chronic infusion of saline or LEV (n = 21–30 mice per genotype and treatment) in the open field and elevated plus maze at 4–6 mo of age. LEV treatment reversed the abnormal increase in ambulations of hAPP mice in the periphery of the open field, which accounted for most of their hyperactivity phenotype in this paradigm (Fig. 2C). In the elevated plus maze, saline-treated hAPP mice showed increased overall ambulations (Fig. 2D) and spent more time in the open arms as compared with NTG mice (Fig. 2 E and F and Fig. S3). LEV treatment reversed these behavioral abnormalities in hAPP mice and did not significantly affect the behavior of NTG controls (Fig. 2 E and F and Fig. S3).

Several lines of evidence suggest that abnormal spike activity can interfere transiently with brain functions (25, 26). To explore whether behavioral abnormalities in hAPP mice are dependent on the continual presence of epileptiform discharges, we suppressed epileptic spike frequency in these mice with a single injection of LEV and tested their behavior 2 h later. Transient reduction of abnormal spikes did not acutely reverse their abnormal behaviors in the open field or elevated plus maze (Fig. S4).

Chronic LEV Treatment Improves Learning and Memory in hAPP Mice. To determine if chronic LEV treatment ameliorates cognitive deficits in hAPP mice, we tested hippocampus-dependent learning and memory in NTG and hAPP mice chronically treated with saline or LEV in two paradigms: habituation to a novel environment and the Morris water maze. After 12 d of chronic infusion, context-dependent habituation (learning) and dishabituation (forgetting) were assessed in a novel environment (open field). Independent of treatment, NTG and hAPP mice habituated to the open field, reaching the same level of activity after four trials (Fig. 3A). However, when mice were retested in the same environment after an interval of 7 d, saline-treated hAPP mice, but none of the other groups, showed complete dishabituation to the open field (Fig. 3A) and impairment of memory retention (Fig. 3B). Like saline- and LEV-treated NTG mice, LEV-treated hAPP mice showed no dishabituation (Fig. 3A) and no impairment in long-term memory retention (Fig. 3B), suggesting that LEV improved context-dependent memory or reduced forgetting in hAPP mice.

Spatial learning and memory were then assessed in the Morris water maze in the same groups of mice after 20 d of chronic infusion. In the spatial (hidden-platform) component, LEV-treated hAPP mice learned better and faster than saline-treated hAPP mice but not as well as NTG controls (Fig. 3C and Fig. S5A). All groups of mice learned similarly well in the visibly cued-platform component (Fig. 3C). In a probe trial performed 24 h after completion of the last training trial, only saline-treated hAPP mice were impaired, showing no preference for the target quadrant (Fig. 3D). Swim speeds were similar among all groups of mice during learning and probe trials (Fig. S5 B and C).

To determine whether LEV treatment also improves nonspatial learning and memory, we tested the effect of LEV in an independent cohort of mice in a novel object recognition paradigm. During the training trial, none of the groups showed a preference for one of the objects (Fig. S6). During the test session, all groups of mice except the saline-treated hAPP mice interacted longer and
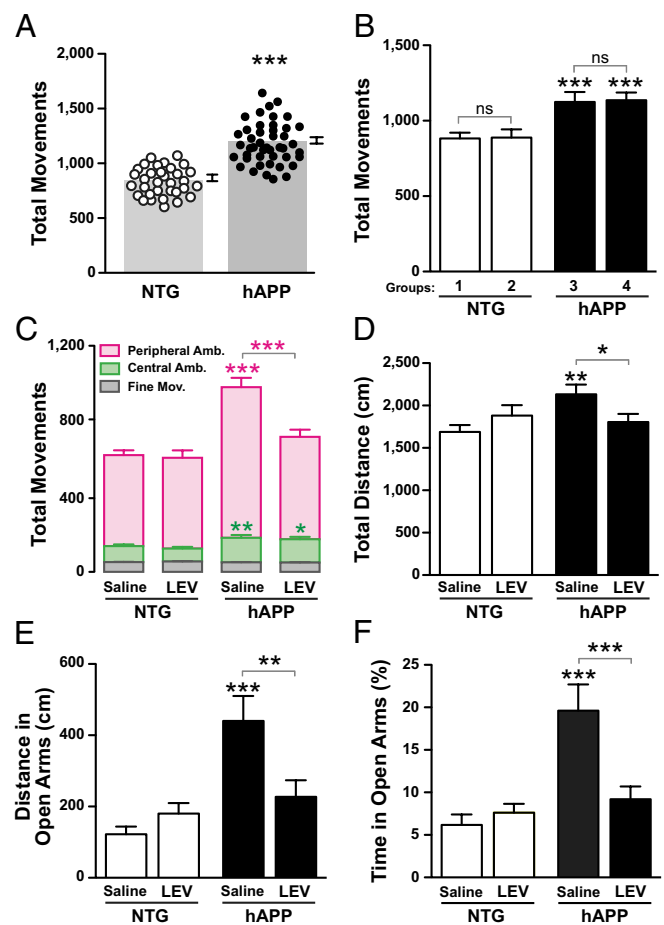

Fig. 2. LEV treatment reverses behavioral abnormalities in hAPP mice. Behavioral testing was performed in two independent cohorts of 4- to 6-mo-old mice. Because results were similar in both cohorts, the data were pooled. (A and B) Before acute and chronic treatments, mice were prescreened in an open field for 5 min. (A) hAPPJ20 mice were more active than NTG controls (***P < 0.0001 by t test). (B) Within each genotype, mice were divided into two groups, so that baseline activity levels did not differ between groups before treatment with LEV or saline. Two-way ANOVA revealed a significant effect of the genotype (P < 0.0001) but not of group (P = 0.61) and no interaction effect (P = 0.43). ***P < 0.0005 vs. NTG (Bonferroni test). (C–F) hAPP mice and NTG controls were treated chronically with saline or LEV (75 mg·kg⁻¹·d⁻¹, s.c.; n = 21–30 mice per genotype and treatment). (C) Mice were tested in the open field 8 d (cohort 1) or 19 d (cohort 2) after the treatment started. The numbers of peripheral and central ambulatory movements and of fine movements were measured. Amb., ambulation; Mov., movements. (D–F) Mice were tested in the elevated plus maze 19 d (cohort 1) or 5 d (cohort 2) after the start of treatment. The total distance moved (D), the distance moved in the open arms (E), and the percentage of total time spent in the open arms (F) were measured. Two-way ANOVA revealed a significant interaction between genotype and treatment [C, P = 0.001 (peripheral ambulation); D, P = 0.007; E, P = 0.003; F, P = 0.012] and a significant genotype effect [C, P = 0.001 (central ambulation)]. *P < 0.05, **P < 0.005, ***P < 0.0005 vs. saline-treated NTG or as indicated by bracket (Bonferroni test). Values are means ± SEM.

more often with the novel object than with the familiar object (Fig. 3 E and F), demonstrating that LEV also improved nonspatial learning and memory in hAPP mice.

Chronic LEV Treatment Reverses Synaptic Deficits in the Hippocampus. Consistent with their hippocampus-dependent memory deficits, hAPP mice show prominent alterations of synaptic functions in the dentate gyrus and hippocampal CA1 region (12, 15, 24, 27). To determine whether chronic LEV treatment improves synaptic
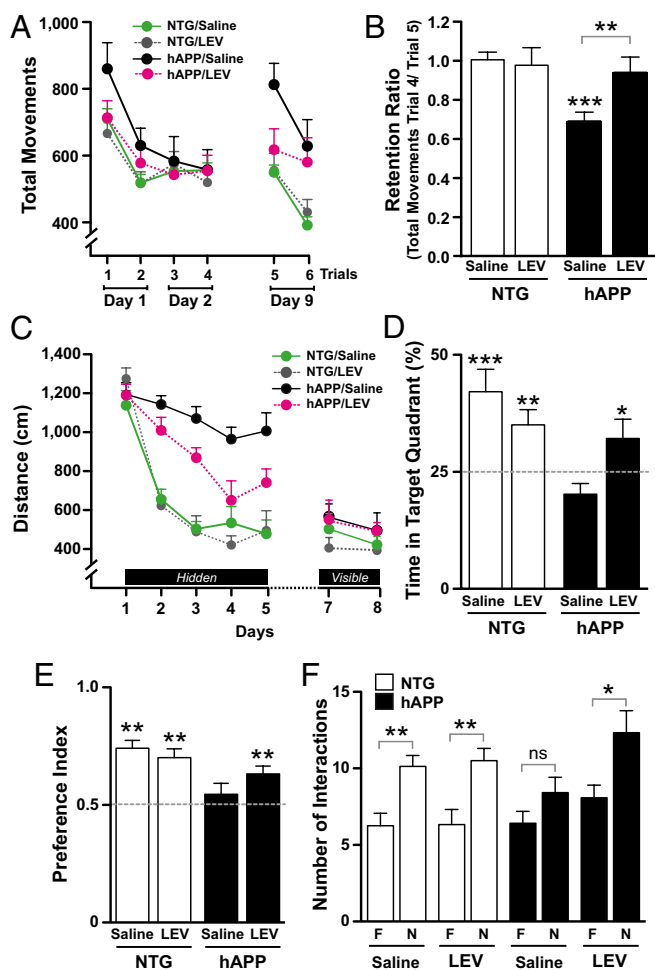
Fig. 3. LEV treatment reverses learning and memory deficits in hAPP mice. hAPPJ20 mice and NTG controls were chronically treated with saline or LEV. (*A*) Context-dependent learning and memory in an open field arena. In the initial phase of this test, all mice (*n* = 10–15 mice per genotype and treatment) showed habituation to the novel environment, reaching similar levels of activity on the fourth trial (no treatment or genotype effects and no interaction by two-way repeated-measures ANOVA). However, when reintroduced into the same arena 7 d later, saline-treated, but not LEV-treated, hAPP mice showed clear evidence of abnormal dishabituation (forgetting) compared with the control groups (*P* = 0.045 for interaction between genotype and treatment on trial 5 by two-way ANOVA). *P* < 0.005 vs. LEV-treated hAPP mice, *P* < 0.0005 vs. saline-treated NTG mice (Bonferroni test). Saline-treated hAPP mice were the only group that showed dishabituation in the open field 7 d after the fourth trial (*P* = 0.006 by paired *t* test, comparing total movements in trial 4 vs. trial 5). (*B*) Spatial learning and memory index (ratio of total movements during trials 4 and 5). Two-way ANOVA revealed a significant interaction between genotype and treatment (*P* = 0.0031). ***P* < 0.0005 vs. saline-treated NTG mice (Bonferroni test). (*C*) Learning curves during spatial training in the Morris water maze (*n* = 10–15 mice per genotype and treatment). The distance each mouse swam to reach the hidden platform was recorded during 5 d. Data points represent the average performance of mice during four training trials/d. Repeated-measures ANCOVA revealed a significant interaction between genotype and day in saline-treated NTG and hAPP mice (*P* = 0.0063) and a significant interaction between LEV treatment and day in hAPP mice (*P* = 0.022) but not in NTG controls. (*D*) Twenty-four hours after the last training session, mice were tested in a probe trial (platform removed), and the percentage of time mice spent swimming in the target quadrant was calculated. One-tailed, one-sample *t* tests were performed to determine if the mean of each group was different from chance (dotted line). **P* < 0.05, ***P* < 0.005, ****P* < 0.0005 vs. 25%. Only saline-treated hAPP mice did not show a preference for the target quadrant. Two-way repeated-measures ANOVA revealed a significant interaction between genotype and treatment (*P* = 0.01). Bonferroni test revealed a significant difference between hAPP/saline and hAPP/LEV

plasticity in the dentate gyrus of hAPP mice, we measured long-term potentiation (LTP) in acute hippocampal slices from 4- to 5-mo-old mice after 20–25 d of LEV treatment. Consistent with previous findings (12, 15, 24, 27), LTP at the perforant path to dentate granule cell synapse was impaired in hAPP mice (Fig. 4 *A* and *B*). Remarkably, chronic LEV treatment fully reversed LTP deficits in hAPP mice (Fig. 4 *A* and *B*). In parallel, we investigated whether LEV also improved synaptic transmission strength, which is impaired in area CA1 of hAPPJ20 mice (12, 15, 24, 27). Comparisons of input/output curves confirmed the deficit in synaptic transmission strength in saline-treated hAPP mice (Fig. 4*C*). Chronic LEV treatment also reversed this deficit (Fig. 4*C*).

Chronic LEV Treatment Reverses Abnormalities in Synaptic Activity-Related Proteins. hAPP mice show changes in diverse synaptic activity-related proteins and prominent remodeling of neuronal circuits in the dentate gyrus (12, 28). Many of these alterations are likely compensatory and may help the dentate gyrus (the "hippocampal gate") prevent cortical spiking activity from spreading into the other subfields of the hippocampal formation. However, as previously suggested, some of the compensatory changes may themselves interfere with normal synaptic functions (12, 28, 29). To determine if chronic reduction of abnormal spike activity reverses alterations in the expression of synaptic activity-related proteins in hAPP mice, we measured expression levels of calbindin, neuropeptide Y (NPY), and Fos in the dentate gyrus of mice treated with saline or LEV for 28 d.

Consistent with previous findings (12, 24, 28), saline-treated hAPP mice had lower levels of calbindin in the molecular layer of the dentate gyrus (Fig. 5 *A* and *D*), higher levels of NPY in mossy fibers (Fig. 5 *B* and *E*), and fewer Fos-positive cells in the granular layer (Fig. 5 *C* and *F*) than saline-treated NTG controls. LEV treatment normalized levels of calbindin (Fig. 5 *A* and *D* and Fig. S7) and NPY (Fig. 5 *B* and *E*) and increased the number of Fos-positive cells in the granular layer (Fig. 5 *C* and *F*) in hAPP mice, supporting the notion that these alterations are triggered and maintained by epileptiform activity.

LEV Does Not Reduce Levels of hAPP, hAPP C-Terminal Fragments, Aβ, or Aβ Deposition in hAPP Mice. Because Aβ production can be influenced by neuronal activity (30–33), we examined whether LEV treatment reduced Aβ levels in brain homogenates and in the interstitial fluid. Aβ levels in the hippocampus of hAPP mice treated with saline or LEV for 20 d were measured by ELISA at 3 mo of age (before formation of amyloid plaques). LEV treatment did not alter Aβ1-x and Aβ1-42 levels or Aβ1-42/Aβ1-x ratios (Fig. 6 *A* and *B*). Chronic LEV treatment also did not change interstitial levels of Aβx-40 and Aβx-42 or Aβx-42/Aβx-40 ratios, as measured by microdialysis in the hippocampus of freely moving 3-mo-old hAPP mice (Fig. 6 *C–F*). LEV treatment also did not affect levels of full-length hAPP and hAPP C-terminal fragments in parietal cortex homogenates (Fig. S8) or early amyloid deposition in the hippocampus and cortex (Fig. S9) of 5- to 6-mo-old hAPP mice.

Behavioral and Molecular Abnormalities Recur Within 35 d After the End of LEV Treatment. To explore whether the beneficial effects of LEV extend beyond the treatment period, we retested mice 35 d

---

(*P* = 0.05). (*E* and *F*) Novel object recognition performed in an independent cohort of mice (*n* = 9–13 mice per genotype and treatment). (*E*) Preference index represents the time spent with the novel object (N) divided by the total time spent with both novel (N) and familiar (F) objects. One-tailed, one-sample *t* tests were performed to determine if the mean of each group was different from chance (dotted line). ***P* < 0.005, vs. 0.5. (*F*) Number of times mice interacted with the novel (N) versus the familiar (F) object during a 10-min test session. **P* < 0.05, ***P* < 0.005 vs. familiar object (unpaired *t* test). Values are means ± SEM.
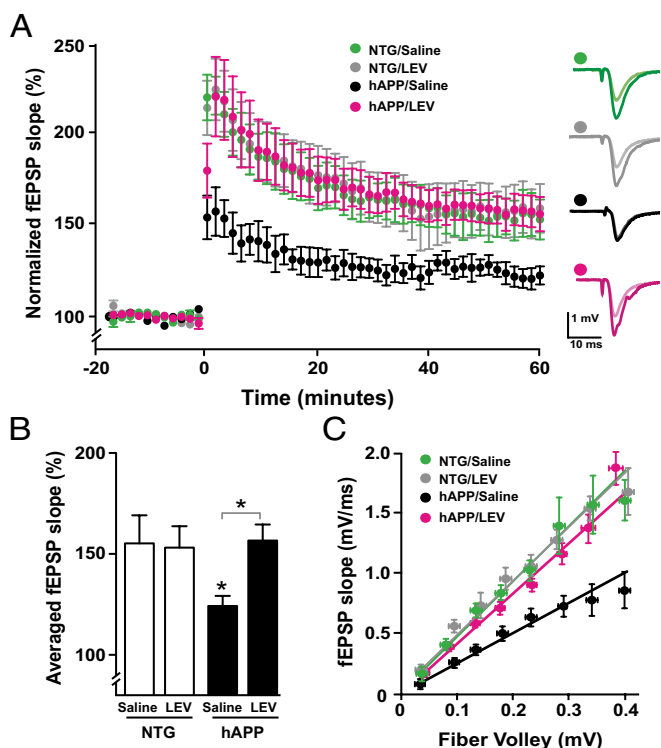
Fig. 4. LEV reverses deficits in synaptic transmission and plasticity in hAPP mice. Field recordings were made from acute hippocampal slices obtained from 4- to 5-mo-old NTG and hAPPJ20 mice treated s.c. with LEV (75 mg·kg^{-1}·d^{-1}) or saline for 20–25 d. (*A* and *B*) LTP induction in the dentate gyrus after theta-burst stimulation of the medial perforant pathway. (*A*) LTP curves illustrate the deficit of synaptic plasticity in saline-treated hAPP mice and the complete reversal of this deficit by LEV treatment. (*B*) Mean of the last 10 min of the LTP recordings. LEV treatment normalized LTP deficits in hAPP mice. Two-way ANOVA revealed a significant interaction between genotype and treatment ($P = 0.045$). *$P < 0.05$ vs. saline-treated NTG or as indicated by bracket (Bonferroni test). Number of slices per number of mice for LTP recordings: NTG/saline, 5/4; NTG/LEV, 4/3; hAPP/saline, 5/5; hAPP/LEV, 7/6. (*C*) LEV reversed synaptic transmission deficits in the CA1 region of hAPP mice. Linear regression analysis of input/output curves revealed that the slope of saline-treated hAPP mice (2.2 ± 0.3) was significantly lower ($P < 0.0001$ by *F*-test) than the slopes of the other groups (NTG/saline, 4.5 ± 0.4; NTG/LEV, 4.2 ± 0.3; hAPP/LEV, 4.4 ± 0.3). Number of slices per number of mice for input/output recordings: NTG/saline, 8/6; NTG/LEV, 5/3; hAPP/saline, 13/7; hAPP/LEV, 10/7. Values are mean ± SEM.

after the s.c. minipump infusions were designed to stop. We first confirmed that LEV was barely detectable in the plasma of hAPP mice at that time (0.17 ± 0.08 μg/mL of plasma). hAPP mice that had been treated with LEV for 28 d showed typical abnormal behaviors in the open field and elevated plus maze 35 d after the putative end of the treatment (Fig. 7 *A* and *B*). These mice had decreased levels of calbindin in the molecular layer and of Fos-positive cells in the granular layer of the dentate gyrus (Fig. 7 *C* and *D*).

Loss of Antiepileptic Efficacy of LEV at High Doses Is Associated with a Loss of Other Beneficial Effects in hAPP Mice. LEV is known to lose antiepileptic efficacy during sustained treatment at high doses in rodents (34–36), presumably because of the development of functional rather than metabolic tolerance (37). A small proportion of patients with epilepsy also develop tolerance to the antiepileptic effects of LEV (37, 38). The mechanisms by which high-dose LEV induces functional tolerance remain unknown (37). We confirmed this tolerance effect in hAPP mice treated with high doses of LEV (150 mg·kg^{-1}·d^{-1} s.c. plus 1.8 mg/mL in drinking water) (Fig. 8*A*). This loss of antiepileptic efficacy

was not caused by a reduction in drug levels, because plasma levels of LEV in hAPP mice treated with the high dose were ~fivefold greater than those in hAPP mice treated with the more efficacious low dose (Fig. 8*B*). To determine whether chronic suppression of abnormal spike activity was required for LEV to exert beneficial effects in hAPP mice, we compared the behavioral performance and molecular alterations in the hippocampus of NTG and hAPP mice chronically treated with saline or LEV at low versus high doses. In contrast to low-dose treatment, high-dose treatment did not reverse behavioral abnormalities (Fig. 8 *C* and *D*) or alterations in the expression of synaptic activity-related proteins (Fig. 8 *E* and *F*). These results are consistent with the finding that LEV improves memory in aged rats with cognitive impairment at low doses but not at high doses (39) and
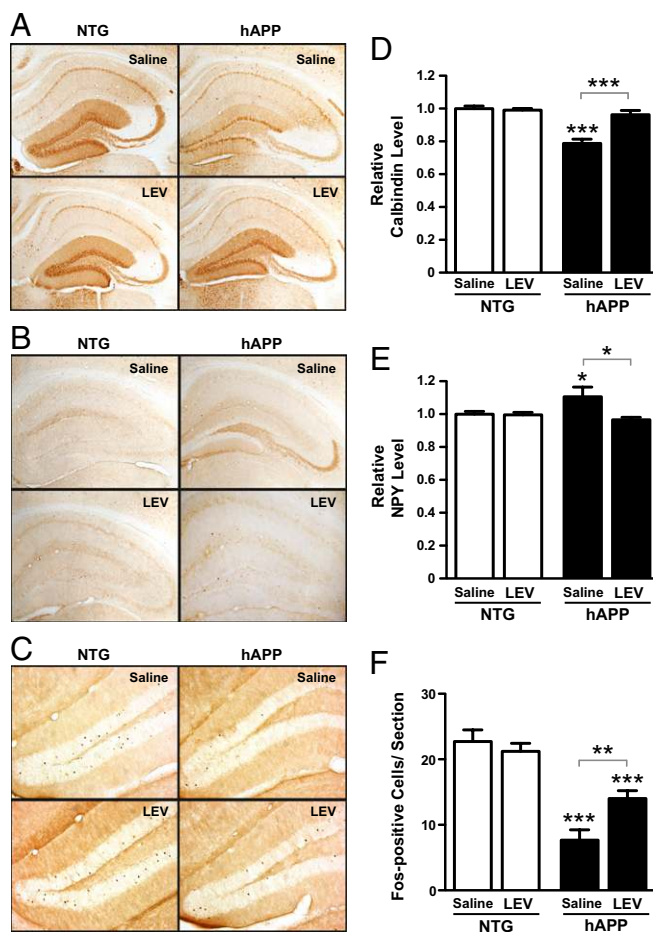

Fig. 5. LEV reverses abnormalities in synaptic activity-related proteins in the dentate gyrus of hAPP mice. Coronal brain sections from NTG and hAPPJ20 mice treated s.c. with saline or LEV (75 mg·kg^{-1}·d^{-1}) for 28 d ($n = 12$–16 mice per genotype and treatment) were immunostained for calbindin, NPY, or Fos. (*A–C*) Photomicrographs illustrating calbindin (*A*), NPY (*B*), and Fos (*C*) alterations in saline-treated hAPP mice and normalization of these biomarkers in LEV-treated hAPP mice. The relative densitometric measures obtained for the sections shown in this figure were 1.06 (NTG/saline), 0.97 (NTG/LEV), 0.71 (hAPP/saline), 1.04 (hAPP/LEV) for calbindin (*A*) and 1.05 (NTG/saline), 0.97 (NTG/LEV), 1.23 (hAPP/saline), 1.01 (hAPP/LEV) for NPY (*B*). (*D* and *E*) Densitometric quantitation of calbindin in the molecular layer of the dentate gyrus (*D*) and of NPY in the mossy fiber pathway (*E*). (*F*) Quantification of Fos-immunoreactive cells in the granular layer of the dentate gyrus. Two-way ANOVA revealed a significant interaction between genotype and treatment: (*D*) $P = 0.0001$; (*E*) $P = 0.029$; (*F*) $P = 0.005$. *$P < 0.05$, **$P < 0.005$, ***$P < 0.0005$ vs. saline-treated NTG or as indicated by bracket (Bonferroni test). Values in *D–F* are mean ± SEM.
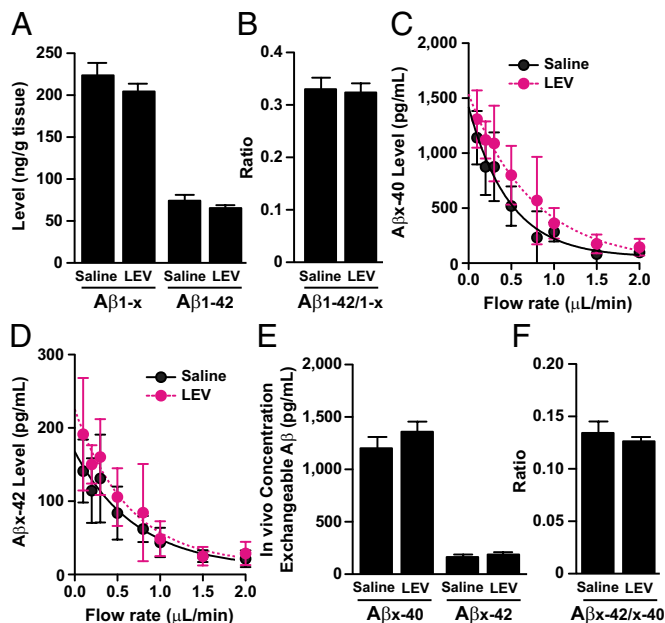
Fig. 6. Prolonged LEV treatment does not alter Aβ levels in the hippocampus of hAPP mice. (A and B) Aβ1-x and Aβ1-42 levels and Aβ1–42/Aβ1-x ratios in the hippocampus of 3-mo-old hAPP mice treated s.c. for 20 d with saline or LEV (75 mg·kg^{-1}·d^{-1}; $n = 8$–9 mice per treatment) were determined by ELISA. LEV treatment did not alter tissue levels of Aβ1-x ($P = 0.8$) or Aβ1-42 ($P = 0.3$) or the Aβ1–42/Aβ1-x ratio ($P = 0.3$). (C–F) Levels of Aβ in the interstitial fluid of the hippocampus were measured by in vivo microdialysis in 5-mo-old hAPP mice treated s.c. for 14 d with saline or LEV (75 mg·kg^{-1}·d^{-1}; $n = 9$ mice per treatment). (C and D) Interpolated zero flow method to quantify the pool of measurable Aβx-40 and Aβx-42 in the hippocampus. (E and F) LEV treatment did not alter exchangeable levels of Aβx-40 ($P = 0.3$) or Aβx-42 ($P = 0.5$) or the Aβx-42/Aβx-42 ratio ($P = 0.5$) by unpaired two-tailed t test. Values are mean ± SEM.

support the hypothesis that the beneficial effects of LEV in hAPP mice depend critically on its antiepileptic activity.

Discussion

Pathologically elevated levels of hAPP/Aβ cause an intriguing combination of cognitive and behavioral alterations, synaptic deficits, and aberrant network activity (3). The results of the current study suggest that aberrant network activity is upstream of and contributes causally to synaptic, cognitive, and behavioral dysfunctions in hAPP mice. Prolonged reduction of abnormal spike activity by chronic LEV treatment ameliorated impairments in learning and memory and fully reversed deficits in synaptic transmission and plasticity in the hippocampus of hAPP mice. In contrast, brief suppression of abnormal spike activity by acute LEV injection failed to improve behavioral abnormalities. These findings raise the intriguing possibility that aberrant network activity contributes to behavioral abnormalities through subacute or chronic mechanisms, such as the remodeling of neuronal circuits and changes in the expression of neuronal gene products. In line with this idea, chronic LEV treatment reversed abnormalities in the expression of neuronal activity-related proteins that reflect hippocampal remodeling and correlate well with cognitive deficits in hAPPJ20 mice (12, 28). In addition, the recurrence of epileptiform activity after the end of the LEV treatment was accompanied by the reappearance of behavioral and molecular abnormalities. Furthermore, at high doses LEV lost both its antiepileptic effect and its beneficial effect on behavioral and molecular abnormalities in hAPP mice.

The most parsimonious interpretation of these findings is that LEV exerts its beneficial effects through the following causal chain: suppression of aberrant network activity, reversal of hippocampal remodeling, and recovery of synaptic and cognitive functions. An alternative interpretation of our results is that synaptic, network, cognitive, and behavioral dysfunctions result from parallel processes triggered by a similar upstream mechanism that is blocked by LEV, for example, glutamate spillover leading to overactivation of extrasynaptic NMDA receptors, a process that has been implicated in ictogenesis (40, 41) and Aβ-induced synaptic dysfunction (42). Additional studies are needed to address these nonexclusive possibilities and the potential relevance of our findings to the human condition.

Although LEV reduced abnormal spike activity in hAPPJ20 mice both acutely and chronically, calcium-channel modulators such as gabapentin and ethosuximide, the GABA analog vigabatrin, and valproic acid, a drug with multiple putative mechanisms of actions, did not show clear antiepileptic efficacy in hAPPJ20 mice, at least at the doses tested here, suggesting that the mechanisms targeted by these drugs may not be critically involved in network dysfunction in this model. Why pregabalin exacerbated epileptiform activity in hAPPJ20 mice is unclear. The sodium-channel blocker phenytoin showed proepileptic effects in APdE9 mice carrying hAPP-Swedish and presenilin-1 mutations (43) and clearly worsened epileptic activity in hAPPJ20 mice (Table 1 and ref. 17). The paradoxical effects of potent
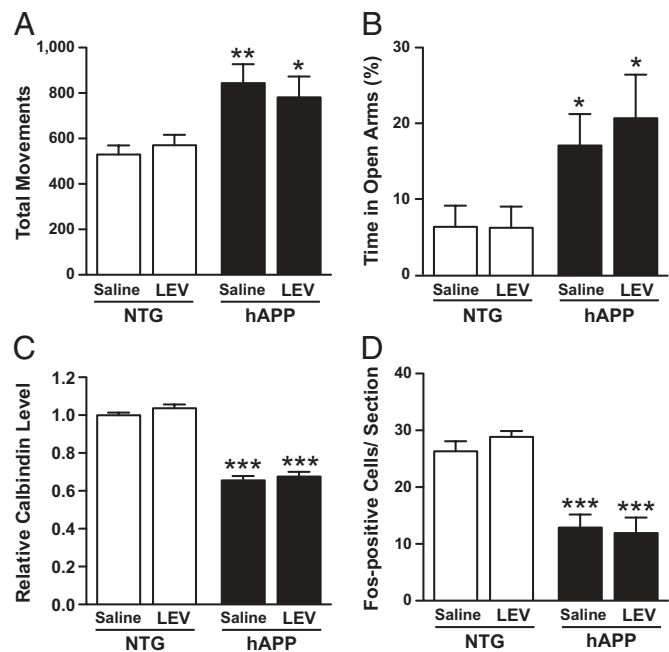

Fig. 7. Behavioral abnormalities and hippocampal remodeling in hAPP mice 35 d after the end of LEV treatment. Four- to six-month-old NTG and hAPPJ20 mice were treated s.c. with saline or LEV (75 mg·kg^{-1}·d^{-1}) for 28 d ($n = 7$–9 mice per genotype and treatment). (A and B) Thirty-five days after the end of the treatment, mice were retested in the open field (A) and the elevated plus maze (B). Two-way ANOVA revealed a significant effect of genotype (A, $P = 0.0009$; B, $P = 0.0054$) but not treatment (A, $P = 0.88$; B, $P = 0.58$) and no interaction between genotype and treatment (A, $P = 0.48$; B, $P = 0.56$). (C and D) Coronal brain sections from these mice were immunostained for calbindin and Fos. Calbindin levels in the molecular layer of the dentate gyrus were quantified by densitometry (C), and the average number of Fos-immunoreactive cells in the granular layer of the dentate gyrus per section was counted (D). Two-way ANOVA revealed a significant effect of genotype (C and D, $P < 0.0001$) but not treatment (C, $P = 0.22$; D, $P = 0.73$) and no interaction between genotype and treatment (C, $P = 0.7$; D, $P = 0.45$). $*P < 0.05$, $**P < 0.005$, $***P < 0.0005$ vs. saline-treated NTG (Bonferroni test). Values are means ± SEM.
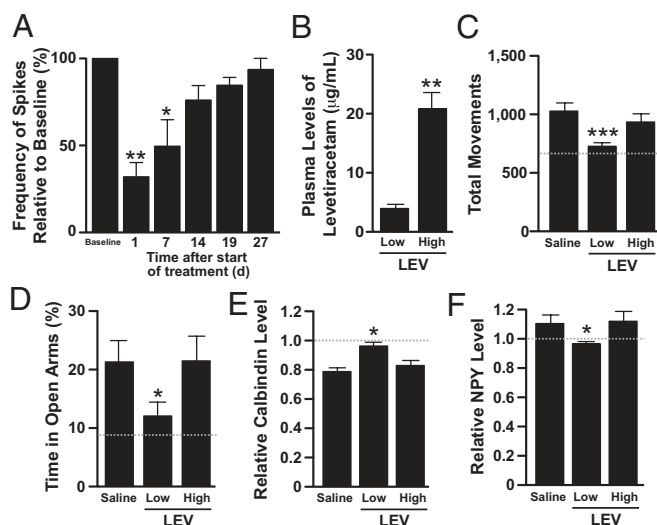
Fig. 8. Loss of antiepileptic efficacy at high doses is associated with a loss of beneficial LEV effects on behavioral and molecular abnormalities in hAPP mice. hAPPJ20 mice were chronically treated with saline or LEV. Two doses of LEV were compared: 75 mg·kg^{-1}·d^{-1} delivered s.c. via implanted osmotic minipumps (low) versus 150 mg·kg^{-1}·d^{-1} delivered s.c. via implanted osmotic minipumps plus LEV added to the drinking water at 1.8 mg/mL (high). (A) EEG activity from parietal cortices was recorded in hAPP mice ($n = 4$) before and during high-dose LEV administration. Loss of efficacy in reducing abnormal spike activity was first observed at 14 d of treatment. *$P < 0.05$, **$P < 0.005$ vs. baseline (one-way ANOVA and Bonferroni test). (B) Plasma concentration of LEV in hAPP mice ($n = 4$) determined after 21 d of chronic infusion of the drug at low versus high doses. **$P < 0.005$ (unpaired t test). (C–F) In an independent cohort of mice, NTG and hAPPJ20 mice were treated with saline or LEV at low or high doses ($n = 10$–15 mice per genotype and treatment). The gray dotted lines in graphs represent the mean of measurements obtained in NTG controls. (C and D) Low-dose but not high-dose LEV reversed the hyperactivity of hAPPJ20 mice in the open field (C) and their disinhibition-like behavior in the elevated plus maze (D). (E and F) Low-dose but not high-dose LEV reversed calbindin depletion in the molecular layer of the dentate gyrus (E) and ectopic expression of NPY in the mossy fibers (F) of hAPP mice. *$P < 0.05$, ***$P < 0.0005$ vs. hAPP treated with saline (one-way ANOVA followed by Bonferroni test). Values are means ± SEM.

sodium-channel blockers in hAPPJ20 mice can be explained, at least in part, by a selective depletion of voltage-gated sodium-channel subunits in inhibitory interneurons of hAPPJ20 mice; such depletion is also observed in humans with AD (17). In line with this interpretation, sodium-channel blockers impair cognition in patients with dementia (44, 45). In contrast, LEV suppressed seizures but did not impair cognitive functions in patients with probable AD and clinically apparent epilepsy (46). Together with our current findings, these observations suggest that LEV may be a better choice than sodium-channel blockers for the treatment or prevention of AD-related neuronal network dysfunction.

The observation that LEV was the only drug tested that was capable of reducing abnormal spike activity in hAPPJ20 mice suggests that suppression of hAPP/Aβ-induced neuronal network dysfunction may depend on a specific activity of LEV. However, the exact mechanism by which LEV counteracts epileptic activity is still uncertain. The antiepileptic efficacy of LEV appears to depend on its binding to the synaptic vesicle protein 2A (SV2A) (47). Although data obtained in neuronal cultures from SV2A-knockout mice suggest that SV2A has a role in the vesicular release machinery (48, 49), it is unclear if and how LEV modifies SV2A function(s). Interestingly, LEV reduces neurotransmitter release in a synaptic activity-dependent manner (50, 51) and particularly in excitatory neurons with a sustained and high frequency of firing (51). In addition, LEV may promote glutamate

uptake by increasing glutamate transporter expression (52). By modulating presynaptic release or glutamate uptake, LEV might prevent excessive glutamate accumulation at the synaptic cleft, preventing overstimulation of postsynaptic glutamate receptors. This mechanism could counteract the pathogenic effects of Aβ, which may cause glutamate spillover at the synaptic cleft as a result of impaired glutamate reuptake (42, 53) and increased glutamate release (54, 55). LEV has additional effects that potentially could counteract pathogenic hAPP/Aβ effects. For example, it reduces calcium release from intracellular stores (56, 57), and this process might help prevent Aβ-induced calcium dysregulation (58, 59).

Convulsive seizures, which occur more frequently in AD patients than in control populations, may represent the tip of an iceberg (3, 7). The incidence of nonconvulsive epileptiform activity and related dysrhythmias in patients with mild cognitive impairment (MCI) and AD is unknown. However, there is plenty of radiological evidence for aberrant network activity in these conditions, including excessive activation of specific nodes. For example, in humans with MCI, functional MRI (fMRI) studies revealed increased activation in AD-vulnerable brain regions during memory tasks (8–11, 60). Although it is unknown if the neural hyperactivation observed in MCI and AD patients is related to abnormal spike activity, it is noteworthy that epileptiform activity in epileptic patients without AD coincides spatially and temporally with focal hyperactivation on fMRI (61–63). In addition, a recent study found that LEV treatment of patients with amnestic MCI, a condition increasingly considered to be an early stage of AD, suppressed aberrant network activity and improved cognitive performance in a hippocampus-dependent task (64). These results are consistent with our findings and suggest that excessive network activity also contributes to cognitive dysfunction in people who are in the process of developing AD.

In conclusion, our study demonstrates that LEV can ameliorate hAPP/Aβ-induced network, synaptic, cognitive, and behavioral dysfunctions. Together, our findings and those of Bakker et al. (64) indicate that targeting aberrant network activity with LEV or related drugs might be of therapeutic benefit in the prevention or treatment of AD. To maximize its therapeutic impact, LEV treatment regimens likely will have to be optimized further with respect to dosage and onset or length of treatment and also may have to be combined with other drugs that complement its mode of action. Because LEV is FDA approved and has a relatively benign side-effect profile, its therapeutic potential deserves to be further explored in additional studies.

Materials and Methods

Transgenic Mice. hAPPJ20 mice (65, 66) were maintained on a C57BL/6J background by crossing heterozygous transgenic mice with NTG C57BL/6J breeders (Jackson Laboratory). Mice had access to food (Picolab Rodent Diet 20; Labdiet) and water ad libitum. Unless indicated otherwise, all the experiments were performed on a sex-balanced group at 4–6 mo of age. The Institutional Animal Care and Use Committee of the University of California, San Francisco, approved all experiments.

Drug Treatments. Levetiracetam (Sequoia Research Products) was dissolved in sterile saline solution (0.9% sodium chloride). For the acute experiments, mice were injected i.p. with saline or various doses of LEV (5, 50, or 200 mg/kg). For the chronic experiments, mice were implanted s.c. in the interscapular region with osmotic minipumps (model 2004; Alzet, Durect). Minipumps were filled with saline or LEV solutions per the manufacturer's instructions. Model 2004 minipumps delivered fluid at a rate of 0.25 μL/h for 28 d. Concentration of LEV in each minipump was calculated to infuse 75 mg·kg^{-1}·d^{-1} or 150 mg·kg^{-1}·d^{-1}. After 24 h of priming in saline solution at 37 °C, minipumps were surgically implanted in mice anesthetized with 3% isoflurane. Mice receiving high-dose LEV were implanted with the minipump infusing 150 mg·kg^{-1}·d^{-1} of LEV and also received LEV in their drinking water (1.8 mg/mL dissolved in tap water). Ethosuximide (Sigma), pregabalin (Sigma), gabapentin (Sigma), vigabatrin (Tocris), and valproic acid (Sigma) were dissolved

in sterile 0.9% sodium chloride; phenytoin was dissolved in sterile PBS. All acute injections were made i.p.

Plasma LEV Levels. A volume of ~50 μL of blood was taken from the facial vein of anesthetized (isoflurane 3%) mice. After centrifugation of blood samples (500 × g for 7 min, 25 °C), plasma was collected and stored at −80 °C. Plasma concentrations of LEV were determined by HPLC with tandem mass spectrometry detection and internal standards (Brainsonline).

EEG Recordings. Mice were implanted for video-EEG monitoring after anesthesia with Avertin (tribromoethanol, 250 mg/kg, i.p.). Teflon-coated silver wire electrodes (0.125-mm diameter) soldered to a multichannel electrical connector were implanted into the subdural space over the left frontal cortex [coordinates relative to the bregma were mediolateral (ML), ±1 mm; anteroposterior (AP), ±1 mm] and the left and right parietal cortex (ML, ±2 mm, AP, ±2 mm). The left frontal cortex electrode was used as a reference. For depth EEG recordings, electrodes were implanted bilaterally into the hippocampus [stereotaxic coordinates: from the bregma, ML, ± 1.66 mm; AP, ± 2.46 mm; from the skull surface, dorsoventral (DV), −1.87 mm]. All EEG recordings were carried out at least 1 wk after surgery on freely moving mice in a recording chamber. Digital EEG activity with video was recorded with the Harmonie software, version 5.0b (Stellate Systems; Natus). Epileptic spikes were detected automatically and scored by the Gotman spike and seizure detectors from Harmonie. EEG traces and videos were inspected systematically for detection of false spikes by an investigator blinded to the treatment and the genotype of the mice. Spike frequency was measured at baseline during 24-h EEG recording in each hAPPJ20 mouse, allowing us to assess the effects of antiepileptic drugs on spike frequency over time within the same mouse.

Behavioral Studies. *Open field.* Spontaneous activity in open field was measured in an automated Flex-Field/Open Field Photobeam Activity System (San Diego Instruments). Before testing, mice were transferred to the testing room and acclimated for 1 h. Mice were tested in a clear plastic chamber (41 × 41 × 30 cm) for 5 min, with two 16 × 16 photobeam arrays detecting horizontal and vertical movements. The apparatus was cleaned with 70% ethanol (by volume) between testing of each mouse. Total movements (ambulatory movements in the center and the periphery and fine movements including rearing) in the open field were recorded for further data analysis. For habituation in the open field (Fig. 3A), mice were retested systematically within the same chamber.
Elevated plus maze. The elevated plus maze consisted of two open and two enclosed arms elevated 63 cm above the ground (Hamilton-Kinder). Mice were allowed to acclimate to the testing room under dim light for 1 h before testing. During testing, mice were placed at the junction between the open and closed arms of the maze and allowed to explore for 5 min. The maze was cleaned with 70% ethanol (by volume) between testing of each mouse. Total distance moved and time spent in both the open and closed arms were calculated for data analysis.
Morris water maze. The Morris water maze test was carried out essentially as described in ref. 27. A full description is given in *SI Materials and Methods*.
Novel object recognition. Mice were transferred to the testing room and acclimated for at least 1 h before testing. They were tested in a white, round, plastic chamber (35 cm in diameter) under dim light. On day 1, mice were habituated to the testing arena for 30 min. On day 2, each mouse was presented with two identical objects in the same chamber and allowed to explore freely for 10 min. On day 3, mice were placed back into the same arena for the test session, during which they were presented with an exact

replica of one of the objects used during training and with a novel, unfamiliar object of different shape and texture. Object locations were kept constant during training and test sessions for any given mouse, but objects were changed semirandomly among mice. Arenas and objects were cleaned with 70% ethanol (by volume) between each mouse. Mice were videotaped, and an investigator blind to their genotype and treatment scored the frequency of interactions and time spent with each object.

Immunohistochemistry. Processing of brain tissues and immunohistochemistry were performed as described (28, 67). Details are given in *SI Materials and Methods*.

Immunoblotting. Western blot analysis was carried out essentially as described in ref. 27. A full description is given in *SI Materials and Methods*.

Electrophysiology on Acute Brain Slices. Slices were prepared from 4- to 5-mo-old NTG and hAPPJ20 mice treated with LEV (75 mg·kg⁻¹·d⁻¹, s.c. osmotic pumps) or saline for 20–25 d. A full description of brain preparation and electrophysiological recordings is given in *SI Materials and Methods*.

ELISA Analysis of Aβ Levels in Brain Tissue. Hippocampi were microdissected and homogenized in 5 M guanidine buffer. Levels of human Aβ1-x and Aβ1-42 were analyzed by ELISA as described (68).

In Vivo Aβ Microdialysis. In vivo microdialysis to assess brain ISF Aβ in the hippocampus of awake, freely moving hAPPJ20 mice was performed as previously described (69, 70). Mice received saline or LEV (75 mg·kg⁻¹·d⁻¹ s.c.) for 2 wk by osmotic minipumps (Alzet; Model 2004). On day 13 or 14 of drug administration, mice underwent in vivo microdialysis to determine absolute levels of ISF Aβ within the hippocampus. Further details are given in *SI Materials and Methods*.

Statistical Analyses. Experimenters who obtained the primary data were blinded as to the genotype and treatment of mice. Statistical analyses were performed with GraphPad Prism version 5.0 or with R. Differences between two means were assessed by unpaired or paired Student's *t* test. Differences among multiple means were assessed, as indicated, by one-way, two-way, or repeated-measures ANOVA, followed by a Bonferroni test. Two-way ANOVA was unidirectional because we hypothesized that LEV reverses abnormalities and dysfunctions in hAPPJ20 mice. Slopes of linear regression curves were compared by F-test using GraphPad Prism version 5.0. To analyze the results of the water maze trials we used a repeated measures analysis of covariance (ANCOVA) to model the distance moved and latency to reach the target, considering genotype (binary variable) and day (continuous variable) as explanatory variables. This specific analysis was done in R with the nlme package. Error bars represent SEM. Null hypotheses were rejected at the 0.05 level.

1. Wimo A, Prince M (2010) *World Alzheimer Report 2010: The Global Economic Impact of Dementia* (Alzheimer's Disease International, London), pp 1–56.
2. Mucke L (2009) Neuroscience: Alzheimer's disease. *Nature* 461:895–897.
3. Palop JJ, Mucke L (2010) Amyloid-beta-induced neuronal dysfunction in Alzheimer's disease: From synapses toward neural networks. *Nat Neurosci* 13:812–818.
4. Golde TE, Schneider LS, Koo EH (2011) Anti-aβ therapeutics in Alzheimer's disease: The need for a paradigm shift. *Neuron* 69:203–213.
5. Huang Y, Mucke L (2012) Alzheimer mechanisms and therapeutic strategies. *Cell* 148:1204–1222.
6. Golde TE, Petrucelli L, Lewis J (2010) Targeting Abeta and tau in Alzheimer's disease, an early interim report. *Exp Neurol* 223:252–266.
7. Palop JJ, Mucke L (2009) Epilepsy and cognitive impairments in Alzheimer disease. *Arch Neurol* 66:435–440.
8. Dickerson BC, et al. (2005) Increased hippocampal activation in mild cognitive impairment compared to normal aging and AD. *Neurology* 65:404–411.
9. Putcha D, et al. (2011) Hippocampal hyperactivation associated with cortical thinning in Alzheimer's disease signature regions in non-demented elderly adults. *J Neurosci* 31:17680–17688.
10. Sperling RA, et al. (2010) Functional alterations in memory networks in early Alzheimer's disease. *Neuromolecular Med* 12:27–43.
11. Celone KA, et al. (2006) Alterations in memory networks in mild cognitive impairment and Alzheimer's disease: An independent component analysis. *J Neurosci* 26:10222–10231.
12. Palop JJ, et al. (2007) Aberrant excitatory neuronal activity and compensatory remodeling of inhibitory hippocampal circuits in mouse models of Alzheimer's disease. *Neuron* 55:697–711.
13. Minkeviciene R, et al. (2009) Amyloid beta-induced neuronal hyperexcitability triggers progressive epilepsy. *J Neurosci* 29:3453–3462.
14. Vogt DL, et al. (2011) Abnormal neuronal networks and seizure susceptibility in mice overexpressing the APP intracellular domain. *Neurobiol Aging* 32:1725–1729.
15. Roberson ED, et al. (2011) Amyloid-β/Fyn-induced synaptic, network, and cognitive impairments depend on tau levels in multiple mouse models of Alzheimer's disease. *J Neurosci* 31:700–711.
16. Harris JA, et al. (2010) Transsynaptic progression of amyloid-β-induced neuronal dysfunction within the entorhinal-hippocampal network. *Neuron* 68:428–441.
17. Verret L, et al. (2012) Inhibitory interneuron deficit links altered network activity and cognitive dysfunction in Alzheimer model. *Cell* 149:708–721.

18. Bialer M, White HS (2010) Key factors in the discovery and development of new antiepileptic drugs. *Nat Rev Drug Discov* 9:68–82.

19. De Smedt T, Raedt R, Vonck K, Boon P (2007) Levetiracetam: Part II, the clinical profile of a novel anticonvulsant drug. *CNS Drug Rev* 13:57–78.

20. De Smedt T, Raedt R, Vonck K, Boon P (2007) Levetiracetam: The profile of a novel anticonvulsant drug-part I: Preclinical data. *CNS Drug Rev* 13:43–56.

21. Chin J, et al. (2005) Fyn kinase induces synaptic and cognitive impairments in a transgenic mouse model of Alzheimer's disease. *J Neurosci* 25:9694–9703.

22. Roberson ED, et al. (2007) Reducing endogenous tau ameliorates amyloid beta-induced deficits in an Alzheimer's disease mouse model. *Science* 316:750–754.

23. Cheng IH, et al. (2007) Accelerating amyloid-β fibrillization reduces oligomer levels and functional deficits in Alzheimer disease mouse models. *J Biol Chem* 282:23818–23828.

24. Harris JA, et al. (2010) Many neuronal and behavioral impairments in transgenic mouse models of Alzheimer's disease are independent of caspase cleavage of the amyloid precursor protein. *J Neurosci* 30:372–381.

25. Binnie CD (2003) Cognitive impairment during epileptiform discharges: Is it ever justifiable to treat the EEG? *Lancet Neurol* 2:725–730.

26. Kleen JK, Scott RC, Holmes GL, Lenck-Santini PP (2010) Hippocampal interictal spikes disrupt cognition in rats. *Ann Neurol* 67:250–257.

27. Cissé M, et al. (2011) Reversing EphB2 depletion rescues cognitive functions in Alzheimer model. *Nature* 469:47–52.

28. Palop JJ, et al. (2003) Neuronal depletion of calcium-dependent proteins in the dentate gyrus is tightly linked to Alzheimer's disease-related cognitive deficits. *Proc Natl Acad Sci USA* 100:9572–9577.

29. Palop JJ, Chin J, Mucke L (2006) A network dysfunction perspective on neurodegenerative diseases. *Nature* 443:768–773.

30. Kamenetz F, et al. (2003) APP processing and synaptic function. *Neuron* 37:925–937.

31. Cirrito JR, et al. (2005) Synaptic activity regulates interstitial fluid amyloid-β levels in vivo. *Neuron* 48:913–922.

32. Cirrito JR, et al. (2008) Endocytosis is required for synaptic activity-dependent release of amyloid-beta in vivo. *Neuron* 58:42–51.

33. Bero AW, et al. (2011) Neuronal activity regulates the regional vulnerability to amyloid-β deposition. *Nat Neurosci* 14:750–756.

34. Löscher W, Hönack D (2000) Development of tolerance during chronic treatment of kindled rats with the novel antiepileptic drug levetiracetam. *Epilepsia* 41:1499–1506.

35. Glien M, Brandt C, Potschka H, Löscher W (2002) Effects of the novel antiepileptic drug levetiracetam on spontaneous recurrent seizures in the rat pilocarpine model of temporal lobe epilepsy. *Epilepsia* 43:350–357.

36. van Vliet EA, et al. (2008) Development of tolerance to levetiracetam in rats with chronic epilepsy. *Epilepsia* 49:1151–1159.

37. Löscher W, Schmidt D (2006) Experimental and clinical evidence for loss of effect (tolerance) during prolonged treatment with antiepileptic drugs. *Epilepsia* 47:1253–1284.

38. Ben-Menachem E, Edrich P, Van Vleymen B, Sander JW, Schmidt B (2003) Evidence for sustained efficacy of levetiracetam as add-on epilepsy therapy. *Epilepsy Res* 53:57–64.

39. Koh MT, Haberman RP, Foti S, McCown TJ, Gallagher M (2010) Treatment strategies targeting excess hippocampal activity benefit aged rats with cognitive impairment. *Neuropsychopharmacology* 35:1016–1025.

40. Wang XM, Bausch SB (2004) Effects of distinct classes of N-methyl-D-aspartate receptor antagonists on seizures, axonal sprouting and neuronal loss in vitro: Suppression by NR2B-selective antagonists. *Neuropharmacology* 47:1008–1020.

41. Maroso M, et al. (2010) Toll-like receptor 4 and high-mobility group box-1 are involved in ictogenesis and can be targeted to reduce seizures. *Nat Med* 16:413–419.

42. Li S, et al. (2011) Soluble Aβ oligomers inhibit long-term potentiation through a mechanism involving excessive activation of extrasynaptic NR2B-containing NMDA receptors. *J Neurosci* 31:6627–6638.

43. Ziyatdinova S, et al. (2011) Spontaneous epileptiform discharges in a mouse model of Alzheimer's disease are suppressed by antiepileptic drugs that block sodium channels. *Epilepsy Res* 94:75–85.

44. Kwan P, Brodie MJ (2001) Neuropsychological effects of epilepsy and antiepileptic drugs. *Lancet* 357:216–222.

45. Mendez M, Lim G (2003) Seizures in elderly patients with dementia: Epidemiology and management. *Drugs Aging* 20:791–803.

46. Cumbo E, Ligori LD (2010) Levetiracetam, lamotrigine, and phenobarbital in patients with epileptic seizures and Alzheimer's disease. *Epilepsy Behav* 17:461–466.

47. Lynch BA, et al. (2004) The synaptic vesicle protein SV2A is the binding site for the antiepileptic drug levetiracetam. *Proc Natl Acad Sci USA* 101:9861–9866.

48. Custer KL, Austin NS, Sullivan JM, Bajjalieh SM (2006) Synaptic vesicle protein 2 enhances release probability at quiescent synapses. *J Neurosci* 26:1303–1313.

49. Chang WP, Südhof TC (2009) SV2 renders primed synaptic vesicles competent for Ca2+ -induced exocytosis. *J Neurosci* 29:883–897.

50. Yang XF, Rothman SM (2009) Levetiracetam has a time- and stimulation-dependent effect on synaptic transmission. *Seizure* 18:615–619.

51. Meehan AL, Yang X, McAdams BD, Yuan L, Rothman SM (2011) A new mechanism for antiepileptic drug action: Vesicular entry may mediate the effects of levetiracetam. *J Neurophysiol* 106:1227–1239.

52. Ueda Y, et al. (2007) Effect of levetiracetam on molecular regulation of hippocampal glutamate and GABA transporters in rats with chronic seizures induced by amygdalar FeCl3 injection. *Brain Res* 1151:55–61.

53. Li S, et al. (2009) Soluble oligomers of amyloid β protein facilitate hippocampal long-term depression by disrupting neuronal glutamate uptake. *Neuron* 62:788–801.

54. Abramov E, et al. (2009) Amyloid-beta as a positive endogenous regulator of release probability at hippocampal synapses. *Nat Neurosci* 12:1567–1576.

55. Kabogo D, Rauw G, Amritraj A, Baker G, Kar S (2010) ß-amyloid-related peptides potentiate K+-evoked glutamate release from adult rat hippocampal slices. *Neurobiol Aging* 31:1164–1172.

56. Angehagen M, et al. (2003) Levetiracetam reduces caffeine-induced Ca2+ transients and epileptiform potentials in hippocampal neurons. *Neuroreport* 14:471–475.

57. Lyseng-Williamson KA (2011) Levetiracetam: A review of its use in epilepsy. *Drugs* 71:489–514.

58. Supnet C, Bezprozvanny I (2010) The dysregulation of intracellular calcium in Alzheimer disease. *Cell Calcium* 47:183–189.

59. Bezprozvanny I (2009) Calcium signaling and neurodegenerative diseases. *Trends Mol Med* 15:89–100.

60. Sperling RA, et al. (2009) Amyloid deposition is associated with impaired default network function in older persons without dementia. *Neuron* 63:178–188.

61. Krakow K, et al. (1999) EEG-triggered functional MRI of interictal epileptiform activity in patients with partial seizures. *Brain* 122:1679–1688.

62. Bénar CG, et al. (2006) EEG-fMRI of epileptic spikes: Concordance with EEG source localization and intracranial EEG. *Neuroimage* 30:1161–1170.

63. Kobayashi E, et al. (2006) Temporal and extratemporal BOLD responses to temporal lobe interictal spikes. *Epilepsia* 47:343–354.

64. Bakker A, et al. (2012) Reduction of hippocampal hyperactivity improves cognition in amnestic mild cognitive impairment. *Neuron* 74:467–474.

65. Rockenstein EM, et al. (1995) Levels and alternative splicing of amyloid β protein precursor (APP) transcripts in brains of APP transgenic mice and humans with Alzheimer's disease. *J Biol Chem* 270:28257–28267.

66. Mucke L, et al. (2000) High-level neuronal expression of abeta 1-42 in wild-type human amyloid protein precursor transgenic mice: Synaptotoxicity without plaque formation. *J Neurosci* 20:4050–4058.

67. Palop JJ, Mucke L, Roberson ED (2011) Quantifying biomarkers of cognitive dysfunction and neuronal network hyperexcitability in mouse models of Alzheimer's disease: Depletion of calcium-dependent proteins and inhibitory hippocampal remodeling. *Methods Mol Biol* 670:245–262.

68. Johnson-Wood K, et al. (1997) Amyloid precursor protein processing and A β42 deposition in a transgenic mouse model of Alzheimer disease. *Proc Natl Acad Sci USA* 94:1550–1555.

69. Cirrito JR, et al. (2003) In vivo assessment of brain interstitial fluid with microdialysis reveals plaque-associated changes in amyloid-beta metabolism and half-life. *J Neurosci* 23:8844–8853.

70. Verges DK, Restivo JL, Goebel WD, Holtzman DM, Cirrito JR (2011) Opposing synaptic regulation of amyloid-β metabolism by NMDA receptors in vivo. *J Neurosci* 31:11328–11337.